GT2017-64420

A NUMERICAL STUDY OF ETHANOL-WATER DROPLET EVAPORATION

Giandomenico Lupo[*]
Department of Mechanics
KTH Royal Institute of Technology
SE-100 44 Stockholm, Sweden
Email: gianlupo@mech.kth.se

Christophe Duwig
Department of Mechanics
KTH Royal Institute of Technology
SE-100 44 Stockholm, Sweden

The present effort focuses on detailed numerical modelling of the evaporation of an ethanol-water droplet. The model intends to capture all relevant details of the process: it includes species and heat transport in the liquid and gas phases, and detailed thermo-physical and transport properties, varying with both temperature and composition. Special attention is reserved to the composition range near and below the ethanol/water azeotrope point at ambient pressure. For this case, a significant fraction of the droplet lifetime exhibits evaporation dynamics similar to those of a pure droplet. The results are analysed and model simplifications are examined. In particular, the assumptions of constant liquid properties, homogeneous liquid phase composition and no differential volatility may not be valid depending on the initial droplet temperature.

Keywords: Droplet; Biofuel; Spray combustion; Multicomponent evaporation

NOMENCLATURE
r Radial coordinate.
d Diameter.
K Evaporation rate constant (d^2-law).
t Time.
T Temperature.
P Pressure.
x Mole fraction in the liquid.
y Mole fraction in the gas mixture.

$\tilde{y}$ Mole fraction in the evaporating mixture.
$\dot{m}$ Evaporation rate.
$\dot{q}$ Heat transfer rate.
D Binary diffusion coefficient.
k Thermal conductivity.
c_p Specific heat at constant pressure.
B_M Spalding mass transfer number.
A_r Averaging parameter.
Le Lewis number.
VLE   Vapour-Liquid Equilibrium

Greek Letters
ω Normalized radial coordinate in the liquid.
ξ Normalized droplet radius.
ρ Density.
α Thermal diffusivity.
ε Fractional evaporation rate.
Λ Latent heat of vaporization.
$\hat{\phi}$ Fugacity coefficient.
γ Activity coefficient.

Subscripts
s Droplet surface.
∞ Infinity.
l Liquid.
g Gas mixture.
V Vapour mixture.
inert   Inert gas.
i Species i.
A Ethanol.
B Water.
0 Initial condition.

---

[*]Address all correspondence to this author.

INTRODUCTION

In recent years, the need to reduce the reliance on fossil fuels for energy production and transportation contributes to an ever increasing interest in biofuels [1]. At the same time, the current regulations on pollutant emissions demand a continuous improvement in the design of clean combustion processes, regardless of the nature of the fuel. This calls for a new generation of combustor technology [2, 3]. The diversity of biofuel production processes is reflected in a large variety of fuel outcomes [4], among which some have significally different properties than traditional fossil fuels [5]. In most cases the low selectivity of the production process originates mixtures with several combustible and non-combustible components. Although separation techniques can be used to ensure a standard quality of the fuel, these often reduce the global efficiency of the process, so recently increasing effort is being put into reducing the cost of the refining stages or avoiding them altogether. As a result, flexibility of the combustion technology is a necessity in order to meet the requirements on combustion efficiency and pollutant emissions. To that end, one needs to understand further the combustion of multicomponent liquid biofuels.

In this study, we contribute by investigating the evaporation of hydrous bioethanol droplets. Bioethanol can be produced from a variety of agricultural feedstocks and food waste, allowing for good flexibility with respect to raw material availability [4]. The second generation fermentation processes results in an aqueous mash, and the subsequent distillation can at most yield an ethanol-water mixture at azeotropic composition. Hydrous ethanol consists of an ethanol-water mixture that can be produced by simple distillation, without further dehydration. Despite the fact that current dehydration technology by pressure swing adsorption has made purification comparatively cheap, significant energy savings (up to 3% of the fuel heating value) can be achieved if the step is avoided altogether, in addition to the lowered investment cost [6]. As a consequence, hydrous/raw bioethanol worldwide production is expected to grow in the coming years, due to its attractiveness as a renewable fuel and its lower production costs than anhydrous ethanol [7]. Enabling clean and efficient combustion of hydrous bioethanol requires further understanding, in particular regarding the differential evaporation of the fuel. The evaporation dynamics of the spray droplets play a significant role in determining the ignition delay and flame structure in spray combustion applications, the key parameters being the total and fractional evaporation rates of the fuel components. These are of special importance in most modern burner configurations, like the lean prevaporized premixed (LPP) gas turbine [8]. Evaporation models have been suggested and are available in the literature and exhaustive reviews can be found in [9–14]. However many models rely on strong assumptions that are not necessarily valid for multicomponent evaporation. For instance, most evaporation models implemented 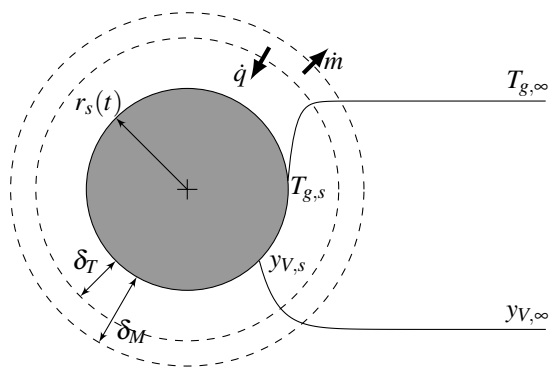in combustion calculations rely on the evaporation rate expression based on the d^2-law [15–17], i.e. assuming steady state evaporation regime of a pure droplet with a prescribed evaporation rate. In fact, the case of multicomponent evaporation has not received much attention and it is unclear which assumptions are valid and how the complex thermodynamics influence the evaporation. To answer these question, we perform detailed numerical simulation of a single droplet evaporation and examine the different potential simplifications. The present paper is structured as follows: detailed presentation of the model, validation for pure fuel evaporation, presentation of the results for different ethanol-water mixtures and discussion on uncertainty and possible simplifications.

FIGURE 1. SKETCH OF THE PROBLEM.

MODEL FORMULATION

We consider the case of a single liquid binary droplet evaporating in an unbounded stagnant gas. Droplet evaporation is driven by the heat transfer from the gas to the liquid phase, and can be sustained by diffusion of the vapour from the droplet surface into the surrounding gas (Fig. 1). The differential volatility of the two components leads to different evaporation rates, thus creating a concentration gradient inside the droplet. The problem is described by the species and heat transport in both the liquid and the gas phase, with phase change controlling the interface dynamics [18]. The thermophysical and transport properties depend on temperature and composition, and henceforth vary in time and space for both phases [19]. Figure 2 qualitatively illustrates the profiles in the liquid and gas phase: as dictated by the thermodynamics, the temperature is continuous at the interface, but with discontinuous derivative, whereas the species mole fraction has a jump across the interface. The following assumptions are made:

1. The system is spherically symmetric.
2. Gravity is neglected.
3. The Soret and Dufour effects are neglected.
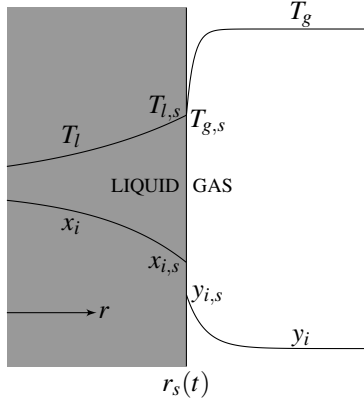4. The gas is ideal.

FIGURE 2. PROFILES IN THE LIQUID AND GAS PHASE.

5. The gas is insoluble in the liquid phase.
6. Heat and mass transport in the gas phase are quasi-steady.
7. Diffusion of the vapour in the gas phase is binary.
8. Thermodynamic equilibrium prevails at the droplet surface.
9. The Kelvin effect on vapour pressure is neglected.
10. The viscous dissipation term and the unsteady pressure term in the gas phase energy equation are neglected.
11. There is no convection in the liquid phase (diffusion-limit transport).
12. Analytical solutions for the species and heat equations are provided for the whole gas domain, but with the following simplifications:

    (a) Pressure varies only inside a thin evaporation layer near the droplet surface (δ_M), and this effect on the momentum transport is considered negligible.
    (b) Evaporation in the layer is isochoric.
    (c) Gas properties are evaluated at a reference temperature and composition that represent averaged values inside the layer.

By assumptions 1 and 2, the range of applicability of the model is limited to very small droplets, which is often the case of spray combustion applications. Assumption 6 will be addressed in the validation section. A full multicomponent species diffusion model is out of the scope of this work, hence we treat the diffusion in the gas as binary Fickian diffusion of the vapour mixture and the inert gas mixture into each other, which is a fair approximation for these mixtures. The Kelvin effect (enhancement of vapour pressure due to surface tension and curvature) was taken into consideration and found to be negligible. The restriction to small droplets makes the liquid transport mechanism purely diffusive, as shear-induced and buoyancy-induced liquid circulation are ruled out by the spherical symmetry and absence of gravity respectively. Observations on assumption 12 are made in the following sections on gas phase and vapour-liquid equilib-

rium modelling.

We stress that the framework outlined by the stated assumptions, i.e. looking at the vaporization dynamics after atomization and before combustion, is mainly relevant for applications such as LPP gas turbines. Therefore variation of properties like liquid viscosity and surface tension does not happen during the liquid break-up/atomization stage, when said properties are of key importance, and has been neglected during the following evaporation stage.

Governing equations

Based on the previously stated assumptions, the system is described by the following equations.

Liquid Phase. As the droplet radius undergoes continuous change due to the evaporation, it is convenient to define a radial coordinate ω, normalized with respect to the droplet radius $r_s(t)$ at each instant:

$$\omega = \frac{r}{r_{s0}\,\xi(t)}, \quad 0 \le \omega \le 1; \tag{1a}$$

$$\xi(t) = \frac{r_s(t)}{r_{s0}}; \tag{1b}$$

where ξ is the droplet radius normalized with its inital value.

Species transport:

$$\frac{r_{s0}^2}{D_{AB}}\xi^2\frac{\partial x_A}{\partial t} = \frac{\partial^2 x_A}{\partial \omega^2} + \left(\frac{2}{\omega} + \frac{1}{\rho_l}\frac{\partial \rho_l}{\partial \omega} + \frac{1}{D_{AB}}\frac{\partial D_{AB}}{\partial \omega} + \frac{1}{2}\frac{r_{s0}^2}{D_{AB}}\omega\frac{\mathrm{d}\xi^2}{\mathrm{d}t}\right)\frac{\partial x_A}{\partial \omega}. \tag{2}$$

Temperature equation:

$$\frac{r_{s0}^2}{\alpha_l}\xi^2\frac{\partial T_l}{\partial t} = \frac{\partial^2 T_l}{\partial \omega^2} + \left(\frac{2}{\omega} + \frac{1}{k_l}\frac{\partial k_l}{\partial \omega} + \frac{1}{2}\frac{r_{s0}^2}{\alpha_l}\omega\frac{\mathrm{d}\xi^2}{\mathrm{d}t}\right)\frac{\partial T_l}{\partial \omega}. \tag{3}$$

The two equations are fully coupled by the dependence of the properties on temperature T_l and mole fraction x_A, and are both tied to the evolution of the normalized droplet surface ξ^2. This follows from the droplet mass balance:

Droplet mass balance:

$$\frac{\mathrm{d}\xi^2}{\mathrm{d}t} = -2\frac{\dfrac{\dot{m}}{4\pi r_{s0}^2}\dfrac{1}{r_{s0}\xi} + \xi^2\displaystyle\int_0^1\omega^2\frac{\partial \rho_l}{\partial t}\mathrm{d}\omega}{\rho_l(\omega=1,t) - \displaystyle\int_0^1\omega^3\frac{\partial \rho_l}{\partial \omega}\mathrm{d}\omega}. \tag{4}$$

3

Equation (4) shows that the evolution of the liquid density can affect the droplet history: for instance if the heatup is very fast, droplet dilatation may lead to a transient increase of the droplet diameter even during evaporation. One may further distinguish between the density change due to temperature and to composition, so that the surface rate of change is driven by three terms: the phase change contribution α and the density change contributions β_T and β_x:

$$\frac{d\xi^2}{dt} = \alpha(\xi,t) + \beta_T(\xi,t) + \beta_x(\xi,t); \tag{5a}$$

$$\alpha(\xi,t) = -\frac{2}{\Psi} \frac{\dot{m}}{4\pi r_{s0}^2} \frac{1}{r_{s0}\xi}; \tag{5b}$$

$$\beta_T(\xi,t) = -2\frac{\xi^2}{\Psi} \int_0^1 \omega^2 \frac{\partial \rho_l}{\partial T_l} \frac{\partial T_l}{\partial t} d\omega; \tag{5c}$$

$$\beta_x(\xi,t) = -2\frac{\xi^2}{\Psi} \int_0^1 \omega^2 \frac{\partial \rho_l}{\partial x_A} \frac{\partial x_A}{\partial t} d\omega; \tag{5d}$$

$$\Psi = \rho_l(\omega=1,t) - \int_0^1 \omega^3 \frac{\partial \rho_l}{\partial \omega} d\omega. \tag{5e}$$

Here α depletes mass from the droplet (assuming $\dot{m} > 0$) and we can expect it to be the main driving mechanism for Eqn. 4 throughout the droplet lifetime. As for β_T and β_x, the mechanisms of diffusive transport in the liquid are usually characterized by significantly different time scales, heat conduction being faster than species diffusion (by one or two orders of magnitude). We can expect the temperature gradient inside the droplet to be extinct after an initial time of order r_{s0}^2/α_{l0}. Thereafter all the heat provided by the gas to the droplet will drive the evaporation as latent heat (see Eqn. 12b), icreasing α at the expense of β_T. On the other hand β_x is tied to the fractional evaporation rate of the vapour species, and is thus controlled by the slow diffusion process in the liquid phase.

Gas Phase. The assumptions made for the gas phase, namely the quasi-steadiness and reference state for evaluation of the properties, allow us to integrate analytically the continuity, species and temperature equations to obtain closed expressions for the total and fractional evaporation rates $\dot{m}$ and ε_i (where $\dot{m}_i = \varepsilon_i \dot{m}$, and $\varepsilon_A + \varepsilon_B = 1$), and the heat transfer rate $\dot{q}$. We define the Spalding mass transfer number B_M for the combined vapour species:

$$B_M = \frac{y_{V,s} - y_{V,\infty}}{1 - y_{V,s}}; \tag{6a}$$

$$y_V = y_A + y_B. \tag{6b}$$

Evaporation rate:

$$\dot{m} = 4\pi \overline{\rho}_g \overline{D}_{V,g} r_s \ln(1 + B_M); \tag{7}$$

$$\varepsilon_i = y_{i,s} + \frac{1}{B_M}(y_{i,s} - y_{i,\infty}); \quad i = A, B. \tag{8}$$

Heat transfer rate:

$$\dot{q} = \frac{\dot{m} Le \, \overline{c}_{p,g}(T_{g,\infty} - T_{g,s})}{F(B_M)}; \tag{9a}$$

$$F(B_M) = \int_1^{1+B_M} s^{(1/Le)-1} \exp\left[\frac{1}{Le}\left(\frac{\overline{c}_{p,V} - \overline{c}_{p,inert}}{\overline{c}_{p,g}}\right)(1 - y_{V,s})(s-1)\right] ds. \tag{9b}$$

The exponential term in Eqn. (9b) comes from the enthalpy diffusion term in the gas heat equation [20], which is the net enthaply flux resulting from the different heat capacities that vapour and inert gas carry with themselves as they diffuse into each other. The term vanishes if $\overline{c}_{p,V} = \overline{c}_{p,inert}$, in which case $\dot{q} = \frac{\dot{m} \overline{c}_{p,g}(T_{g,\infty} - T_{g,s})}{(1+B_M)^{1/Le} - 1}$. This is an established approximation [9–14, 21–25], that will be examined in the validation section.

The average gas phase properties in Eqn. (7) and (9) are evaluated at a reference temperature and composition:

$$T_{g,\text{ref}} = T_{g,s} + A_r(T_{g,\infty} + T_{g,s}); \tag{10a}$$

$$y_{V,\text{ref}} = y_{V,s} + A_r(y_{V,\infty} + y_{V,s}). \tag{10b}$$

We here follow the $A_r = 1/3$ rule, which has been shown to yield the best predictions for a wide range of conditions [12, 26].

Boundary Conditions. At the droplet center we impose symmetry boundary conditions:

$$\left.\frac{\partial x_A}{\partial \omega}\right|_{\omega=0} = 0; \quad \left.\frac{\partial T_l}{\partial \omega}\right|_{\omega=0} = 0. \tag{11}$$

The boundary conditions at the droplet surface establish the coupling between liquid and gas phase:

$$\left.\frac{\partial x_A}{\partial \omega}\right|_{\omega=1} = \frac{\dot{m}}{4\pi r_{s0}\xi \rho_{l,s} D_{AB,s}}(x_{A,s} - \varepsilon_A). \tag{12a}$$

$$\left.\frac{\partial T_l}{\partial \omega}\right|_{\omega=1} = \frac{1}{4\pi r_{s0}\xi k_{l,s}}\left(\dot{q} - \dot{m}\sum_{i=A,B}\varepsilon_i \Lambda_i\right). \tag{12b}$$